# Generating Controlled Molecular Gradients in 3D Gels

**W.J. Rosoff,[1] R. McAllister,[2] M.A. Esrick,[2] G.J. Goodhill,[1] J.S. Urbach[2]**

*[1]Department of Neuroscience, Georgetown University Medical Center, Washington, DC 20007*
*[2]Department of Physics, Georgetown University, Washington, DC 20057; telephone: (202) 687-6584; fax: (202) 687-2087; e-mail: urbach@physics.georgetown.edu*

*Received 3 January 2005; accepted 15 March 2005*

*Published online 24 June 2005 in Wiley InterScience (www.interscience.wiley.com). DOI: 10.1002/bit.20564*

**Abstract:** A new method for producing molecular gradients of arbitrary shape in thin three dimensional gels is described. Patterns are produced on the surface of the gel by printing with a micropump that dispenses small droplets of solution at controlled rates. The molecules in the solution rapidly diffuse into the gel and create a smooth concentration profile that is independent of depth. The pattern is relatively stable for long times, and its evolution can be accurately described by finite element modeling of the diffusion equation. As a demonstration of the method, direct measurements of protein gradients are performed by quantitative fluorescence microscopy. A complementary technique for measuring diffusion coefficients is also presented. This rapid, flexible, contactless approach to gradient generation is ideally suited for cell culture experiments to investigate the role of gradients of diffusible substances in processes such as chemotaxis, morphogenesis, and pattern formation, as well as for high-throughput screening of system responses to a wide range of chemical concentrations.

**Keywords:** cell motility assay; molecular gradients; collagen gel; diffusible factors

## INTRODUCTION

Many important biological processes, such as morphogenesis (Gurdon and Bourillot, 2001) and chemotaxis (Parent and Devreotes, 1999), rely on gradients of molecular factors that are established by diffusion. To study these processes in vitro, a variety of techniques have been developed for producing gradients of chemical factors in three-dimensional gels. The simplest approach is to place the gel in contact with a chamber of solution or gel containing the factor of interest. Diffusion of the factor creates a continuously evolving gradient (Knapp et al., 1999; Letourneau, 1978; Moghe et al., 1995). A more controlled gradient can be produced by placing a gel between two chambers with differing concentrations of factor. After an initial transient, a linear gradient is established between the two chambers (Cao and Shoichet, 2001; Fisher et al., 1989; Haddox et al., 1991; Nelson et al., 1975). The main drawbacks of this method are that the gradient is established only after an initial transient that can be fairly long for large proteins and other slowly diffusing molecules, the reservoirs require a large excess of chemical factor, only linear gradients can be produced, and a separate apparatus is required for each culture dish. Protein gradients have also been incapsulated in a microporous gel by creating a linear gradient in a mold before gelation (Kapur and Shoichet, 2004). There are many approaches for producing gradients on surfaces (Kramer et al., 2004; Ruardy et al., 1997) and recently an elegant method for generating complex gradient shapes in solution and on surfaces using micro fluidics has been demonstrated (Dertinger et al., 2001), but these technologies are not suitable for investigating many biological processes that occur in three-dimensional environments.

We have developed a technique for gradient generation that relies on a computer-controlled micropump to create patterns of chemical factors on the surface of a relatively thin gel. As detailed below, this approach offers several significant advantages over most existing methods: There is no contact between the micropump and the gel, gradients can easily be reproduced in multiple experimental chambers, a variety of gradient shapes can be generated with the same hardware, no excess factor is required, and the gradients are established quickly. The shape of the gradients evolves in time in a way that can be accurately modeled by the diffusion equation. This evolution is the main drawback of this method compared to those described above, which can produce nearly stable gradients after sufficient time. As shown below, however, the slow diffusion of many large proteins results in gradients that are surprisingly stable for a day or more, which is adequate time for many in vitro studies. In particular, we have employed this technique to produce precise measurements of the response of developing axons to precisely controlled gradients of diffusible neurotrophic factors, and found that they are among nature's most sensitive gradient detectors (Rosoff et al., 2004). In cases where greater stability

*Correspondence to:* J.S. Urbach
Contract grant sponsors: NSF; NIH; The Whitaker Foundation

is needed, gradients created by this method can be immobilized by photochemically binding the proteins to the gel matrix (e.g. Cao and Shoichet, 2002; Kapur and Shoichet, 2003).

## MATERIALS AND METHODS

### Collagen Gel Preparation

A 2 mg/mL collagen gel solution was prepared under sterile conditions by mixing on ice type I rat tail collagen stock (Collaborative Biomedical Products, Bedford, MA) diluted with water to contain 2 mg/ml collagen, 27 μL of a 7.5% sodium bicarbonate solution per mL of original collagen stock, and 1/10 final volume of 10× OptiMEM (Invitrogen, Carlsbad, CA). 1,500 μL of the solution was placed in a 35 mm dish spread uniformly over the bottom of the dish, forming a layer of collagen approximately 1 mm thick. The dishes were placed in an incubator until the gel set.

### Pattern Printing

The printing was performed by a commercially available pump (Gesim) that can deliver precisely repeatable nanoliter droplets at programmable rates of up to 1,000 drops per second. A dish containing the gel was mounted on a computer controlled commercial high precision x–y translation stage (Velmex Inc., Bloomfield, NY). The spacing between drops was controlled by varying the rate of droplet ejection and the rate of translation of the x–y stage. The motion of the translation stage and the droplet ejection was controlled by Labview software (National Instruments, Austin, TX). A diagram of the printing system is shown in Figure 1. (An integrated system for complex pattern generation, the Nanoplotter, is also available from Gesim and can perform similar functions.) For most runs, the translation stages moved at 2 mm/s and the droplet ejection rate varied between 15 and 100 drops/s. In situations where more solution was required, the program would produce multiple passes of the pump over the same line. The initial width of the printed lines is determined by the spreading of the droplets when they hit the surface of the gel. For our experiments with collagen, this spreading was on the order of 0.1 mm.

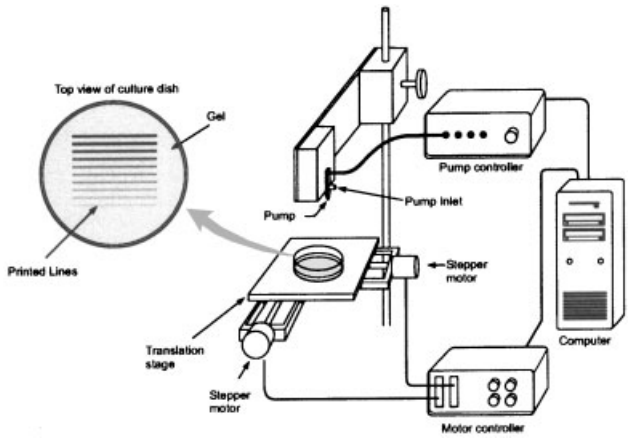


**Figure 1.** Schematic of the gradient generation apparatus. Patterns are printed by moving the gel while droplets are ejected by the pump. The pump and stepper motors are controlled by commands sent via serial ports using a custom program written in LABVIEW (National Instruments).

### Fluoresence Imaging

b-Casein (Sigma, St. Louis), a 24 kDa protein, was labeled with FluoReporter Oregon Green 488 Protein Labeling Kit (Molecular Probes, Eugene, OR), as per the kit instructions. Labeled protein concentration was determined by the Lowry method. Fluorescence intensity was measured by a custom imaging setup built around a Cohu 4922–2010 cooled CCD monochrome camera. The sample was imaged through a telescopic optic with a depth of field greater than the thickness of the collagen.

Standards for calibration were produced by uniformly mixing different concentrations of labeled protein with the collagen solution before the gel was set. A linear calibration of concentration versus intensity was generated from the standards. A background signal measured by imaging a gel with no labeled protein was subtracted from all images before analysis. The sensitivity of the fluorescence imaging may vary with depth because of absorption and scattering. However, this will not affect the calibration curve because the concentration does not vary with depth in the standards or the patterns imaged (see Fig. 4a).

### Simulations of Diffusion

Molecular diffusion was modeled using a three-dimensional finite element modeling program (Femlab v. 3, Comsol) of the diffusion equation to simulate the experimental cylindrical domain, 35 mm in diameter and 1 mm in depth with no-flux boundary conditions. The printing of the diffusant lines was modeled by a nearly constant flux of brief duration (10 s) in narrow regions (0.1 mm). We used the standard Femlab time dependent diffusion model with quadratic elements. The integration meshes of the solutions displayed in Figures 2, 3, and 4 were generated using the fine or extra fine mesh parameter settings, and convergence was tested by examining the stability of solutions as mesh parameters were varied. The number of degrees of freedom in the final meshes ranged between 100,000 and 200,000.

## RESULTS AND DISCUSSION

### Principle of Gradient Generation

Diffusion of large proteins in collagen and other gels is typically quite slow. For example, we have measured the diffusion coeficient, D, of NGF in collagen to be $D_{\mathrm{NGF}} = 8 \times 10^{-7}$ cm$^2$/s (Rosoff et al., 2004). The timescale for significant diffusion along the lateral dimension of an $L =$ 1 cm long culture dish is $\tau \sim L^2/D_{\mathrm{NGF}} \approx 14$ days. This presents something of a challenge for many traditional

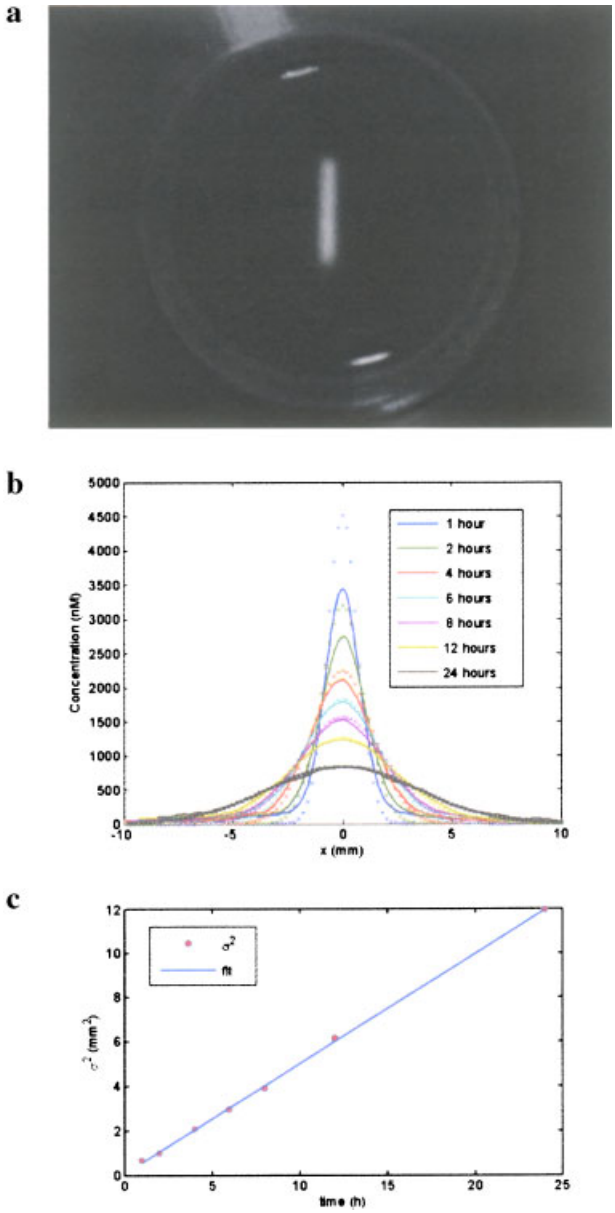


**Figure 2.** Measurement of the diffusion coefficient of fluorescent casein. **a**: A single line printed on a 1 mm thick collagen layer in a 35 mm diameter petri dish, imaged approximately 1 h after printing. **b**: Solid lines: The concentration in the direction perpendicular to the line measured at different times by quantitative fluorescence imaging. Symbols: Concentration profiles derived from numerical solutions to the diffusion equation for the measured value of $D_{casein} = 6.8 \times 10^{-7} cm^2/s$. **c**: Symbols: The square of the standard deviation of Gaussian fits to the fluorescent profile as a function of time. Line: Linear fit, $R^2$=0.99. [Color figure can be seen in the online version of this article, available at www.interscience.wiley.com.]

approaches to gradient generation, because the time necessary for the gradient to stabilize can be prohibitively large. However diffusion acts much more rapidly over short distances. For example, the timescale for NGF to diffuse into the middle of a 1 mm deep gel from the surface is less than an hour. Similarly, fine features on a pattern printed onto the surface of a gel will be rapidly smoothed by molecular diffusion. Thus an arbitrary gradient can be created by printing a pattern of variable concentration onto the surface of a thin

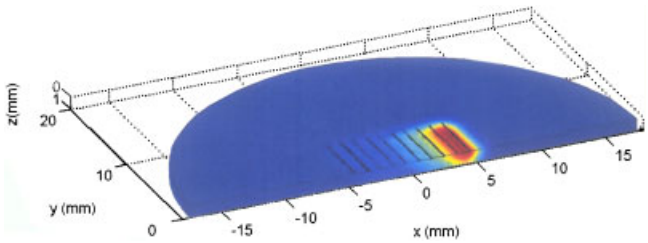


**Figure 3.** Concentration profile generated by simulation of the diffusion equation for an exponential gradient, 1 h after the deposition of 10 lines, 10 mm in length and 1 mm apart, with the amount of factor in each successive line increased by a factor of 1.49. The experimentally determined diffusion coefficient for casein, $D_{casein} = 6.8 \times 10^{-7} cm^2/s$, was used in the simulation. [Color figure can be seen in the online version of this article, available at www.interscience.wiley.com.]

gel, such as a series of thin, equally spaced parallel lines of factor with a regular variation in the concentration from one side of the gel to the other.

## Measurements of Diffusion Coeficients

The timescales for the generation of a smooth concentration profile and for the eventual decay of that profile are proportional to the diffusion coefficient $D$ of the molecular factor in the gel. We have developed a quick and convenient method for directly measuring $D$ in our gels. Using the printer setup, a single 10–20 mm long line of fluorescently labeled molecular factor is delivered onto the middle of a large (35 mm) petri dish containing the gel, such as the line of fluorescently labeled casein, a 24 kDa protein, shown in Figure 2a. (Casein has a molecular weight comparable to NGF, but is relatively inexpensive and easier to label.) The narrow line spreads out into a Gaussian concentration profile and the square of the Gaussian width $\sigma$ (standard deviation) evolves linearly in time, with a slope determined by $D$, $\sigma^2 = 2Dt$ (Crank, 1975). The solid lines in Figure 2b show the concentration profile at different times in the direction perpendicular to the line measured by quantitative fluorescence imaging (see methods). Figure 2c shows $\sigma^2$, determined from fitting each profile to a Gaussian, plotted versus time. The solid line is a linear fit, which gives $D_{casein} = 6.8 \times 10^{-7}$ $cm^2/s$. The symbols in Figure 2b show the result of numerical solutions to the diffusion equation using the measured value of $D$. The agreement at long times is good, while at short times discrepancies are evident. This is probably due to the difficulty of exactly modeling the initial conditions, in particular the exact distribution of dye molecules deposited by the pump, and does not significantly affect the measurement of the diffusion coeficient.

## Molecular Gradients

Concentration patterns of virtually any shape can be produced by controlling the rate of droplet delivery by the pump. After a relatively short time, the concentration of factor in the gel approaches the average density of factor molecules in the immediate vicinity. Figure 3 shows the concentration

profile after 1 h, calculated by a simulation of the diffusion equation for a series of 10 lines, 10 mm in length and 1 mm apart, with the number of drops in each successive line increased by a factor of 1.49. This produces an exponential gradient with a concentration that increases 0.4% every 10 microns. The simulation was performed using the experimentally determined value of $D_{\text{casein}}$. Figure 4a shows the concentration as a function of depth determined from the simulation at various times near the center of the gradient. Because the time for NGF diffusion through the depth of the thin gel is relatively short, the concentration rapidly becomes independent of depth.

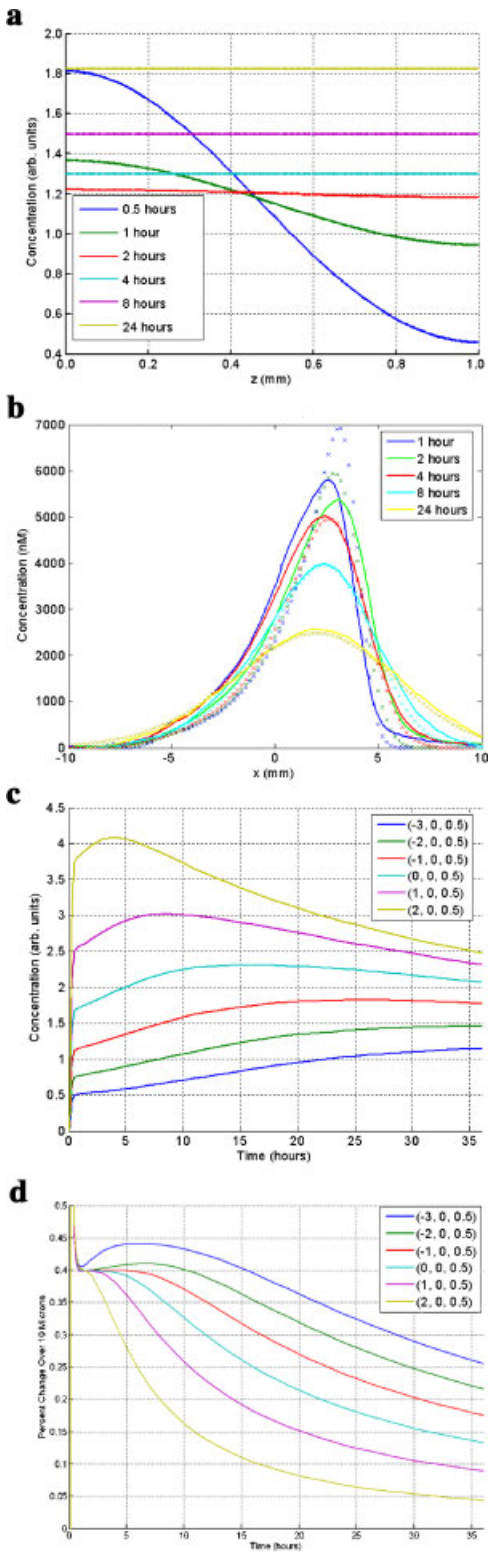


A pattern of fluorescent casein in collagen gel was prepared matching the condition described in the preceding paragraph. In Figure 4b, we compare the measured concentration profiles with the simulations. As with the single line measurements, the agreement at short times is poor, presumably due to the uncertainty about the precise initial concentration distribution as mentioned above. At intermediate and long times the agreement is good.

The concentration at the low end of the gradient rises over time while the concentration at the high end decreases, as a result of diffusion from the high-concentration end. This can be seen in Figure 4c, which shows the concentration as a function of time for several points along the gradient calculated in the simulation. In Figure 4d we plot the percentage change in concentration over a distance of 10 microns, the size of a typical cell. The gradient becomes shallower everywhere along the gradient, but at the lower end of the gradient the change is relatively modest. For shallower gradients, the curves at the low end of the gradient are approximately constant over 24 h (Rosoff et al., 2004). Since the rate of diffusion is proportional to the diffusion coefficient, curves similar to Figure 4c,d for any value of $D$ can be produced simply by rescaling the time axis by the ratio of diffusion coeffficients.

## DISCUSSION

The method for gradient generation we have developed has several significant advantages over previous approaches: large numbers of identical gradients can be generated quickly, the often precious molecular factors are required only in very limited quantities, the gradients are established in a short time, and complex concentration profiles can be generated.

A wide range of two-dimensional concentration profiles can be generated in a thin gel using this approach. The smallest features in the profile must be significantly larger than the precision of the placement of the factor in the initial pattern. In our implementation, this is limited primarily by the spreading of the droplets upon impact with the gel. This

**Figure 4.** Time evolution of the concentration profile. **a**: Concentration profiles through the vertical thickness of the gel at x = −1 mm and y = 0 mm (see Fig. 3), at various times from a numerical solution to the diffusion equation. **b**: Comparison of measured and calculated concentration profiles. Solid lines: The concentration in the direction along the gradient measured at different times by quantitative fluorescence imaging. Symbols: Concentration profiles from the numerical simulation. **c**: Concentration as a function of time produced in the simulation at different points along the gradient. **d**: Gradient strength as a function of time produced in the simulation at different points along the gradient. The legends in (c) and (d) give the (x, y, z) coordinates, using the same coordinate system as Figure 3. The measured value of $D_{casein} = 6.8\times10^{-7}\text{cm}^2/\text{second}$ was used for the numerical calculations. [Color figure can be seen in the online version of this article, available at www.interscience.wiley.com.]

approach can be extended to thicker gels, but the time it takes to reach the depth-independent concentration profiles shown in Figure 4a increases with the square of the gel thickness.

The profile will evolve towards a uniform concentration, unless the factor is fixed in place (e.g., Cao and Shoichet, 2002; Kapur and Shoichet, 2003). The length of time for which the pattern is reasonably stable depends on the details of the pattern. In general, steep gradients and small features are the least stable.

There are several competing constraints that need to be balanced when determining the parameters for generating particular concentration profiles. Droplets ejected too close together tend to coalesce on the surface before diffusing into the gel. In addition, at high enough droplet density the volume of solution may be enough to modify the properties of the gel. In our experiments we have typically limited our linear droplet density to 50 1.4 nL drops per mm. In order for the lines to be well-defined the spacing between droplets within a line should be smaller than the spacing between the lines, which for our experiments is typically 1 mm. Thus a concentration range of up to a factor of 50 is available from a single solution. We have produced patterns with significantly larger ranges of concentrations by changing to a more concentrated solution after printing the low-concentration end of the pattern. (Alternatively, multiple pump heads loaded with different concentrations could be employed.)

The volume of solution deposited is small compared to the volume of the gel, but the variation of droplet density in the printed pattern may produce effects that compete with the effects of the molecular concentration gradient. If this is a concern (as it was in our measurements of the chemotactic response of developing axons, Rosoff et al., 2004), the total volume of fluid deposited on each line can be equalized by the application of an appropriate amount of the buffer after the deposition of the pattern of molecular factor of interest.

There are a number of variations on the approach presented here that might be useful for particular applications. The erosion of the high concentration end of a gradient can be slowed by placing it near an impermeable barrier. A similar effect can be produced by placing two gradients back-to-back, creating a ''ridge'' with identical gradients falling off on each side of the ridge. By symmetry, there is no net flux of molecules between the two gradients, so each evolves as though it were up against an impermeable barrier. This approach is likely to be useful when steep gradients are required. In general diffusion from the high concentration side of the gradient causes the concentration at the low end to rise significantly. This effect can be reduced by shortening the pattern, but the shorter pattern results in a more rapid flattening of the gradient. Because the back-to-back gradients slow the erosion of the high concentration end, two short, steep gradients back to back will optimize the stability in some situations. Numerical simulations of the diffusion equation provide a convenient method for optimizing the initial pattern for a particular application.

We have worked exclusively with 35 diameter circular dishes, but the approach is particularly well suited to rectangular dishes where long lines can be produced, so that samples can be placed far from the edges of the pattern. Another variation is to produce circularly symmetric patterns, e.g. by rotating the gel underneath the pump. A similar geometry is used in the Spiral Gradient Endpoint method for bacterial enumeration (e.g. Hill and Schalkowsky, 1990; Wexler et al., 1996).

This approach completely eliminates edge effects, and has the advantage that, when the high concentration end of the gradient is placed at the center of the dish, there is less factor used and the problem of diffusion to the low concentration parts of the pattern is reduced. However some applications, such as creating multiple gradients in different directions, do not easily adapt to a circular geometry.

In conclusion, we have developed a rapid, flexible, contactless approach to molecular gradient generation in gels. The technique takes advantage of flexible microdispensing technology and the slow diffusion of large proteins. We anticipate that this approach will be useful for studies of chemotaxis, morphogenesis and pattern formation in a variety of systems, as well as for high-throughput screening applications.

We thank Steve Pesanti, Christine Fleury, and Jeff Torri for their assistance with the printing and imaging.

## References

Cao X, Shoichet MS. 2001. Defining the concentration gradient of nerve growth factor for guided neurite outgrowth. Neuroscience 103:831–840.

Cao X, Shoichet MS. 2002. Photoimmobilization of biomolecules within a 3-dimensional hydrogel matrix. J Biomat Sci Plym Edit 13:623–636.

Crank J. 1975. The mathematics of diffusion. Second edn. Oxford: Clarendon Press.

Dertinger SK, Chiu DT, Jeon NL, Whitesides GM. 2001. Generation of gradients having complex shapes using microfluidic networks. Anal Chem 73:1240–1246.

Fisher PR, Merkl R, Gerisch G. 1989. Quantitative analysis of cell motility and chemotaxis in *Dictyostelium dicoideum* by using an image processing system and a novel chemotaxis chamber providing stationary chemical gradients. J Cell Biol 108:973–984.

Gurdon JB, Bourillot PY. 2001. Morphogen gradient interpretation. Nature 413:797–803.

Haddox JL, Pfister RR, Sommers CI. 1991. A visual assay for quantitating neurotrophil chemotaxis in a collagen gel matrix: A novel chemotactic chamber. J Immunol Methods 141:41–52.

Hill GB, Schalkowsky S. 1990. Development and evaluation of the spiral gradient endpoint method for susceptibility testing of anaerobic gram-negative bacilli. Rev Infect Dis 12(Suppl 2):S200–S209.

Kapur TA, Shoichet MS. 2003. Chemically-bound nerve growth factor for neural tissue engineering applications. J Biomater Sci Polym Edn 14: 383–394.

Kapur TA, Shoichet MS. 2004. Immobilized concentration gradients of nerve growth factor guide neurite outgrowth. J Biomed Mater Res A 68:235–243.

Knapp DM, Helou EF, Tranquillo RT. 1999. A fibrin or collagen gel assay for tissue cell chemotaxis: Assessment of fibroblast chemotaxis to GRGDSP. Exp Cell Res 247:543–553.

Kramer S, Xie H, Gaff J, Williamson JR, Tkachenko AG, Nouri N, Feldheim DA, Feldheim DL. 2004. Preparation of protein gradients through the

controlled deposition of protein-nanoparticle conjugates onto functionalized surfaces. J Amer Chem Soc 126:5388–5395.

Letourneau PC. 1978. Chemotactic response of nerve fiber elongation to nerve growth factor. Dev Biol 66:183–196.

Moghe PV, Nelson RD, Tranquillo RT. 1995. Cytokine-stimulated chemotaxis of human neutrophils in a 3-D conjoined fibrin assay. J Immunol Methods 180:193–211.

Nelson RD, Quie PG, Simmons RL. 1975. Chemotaxis under agarose: A new and simple method for measuring chemotaxis and spontaneous migration of human polymorphonuclear leukocytes and monocytes. J Immunol 115:1650–1656.

Parent CA, Devreotes PN. 1999. A cell's sense of direction. Science 284: 765–770.

Ruardy TG, Schakenraad JM, van der Mei HC, Busscher HJ. 1997. Preparation and characterization of chemical gradient surfaces and their application for the study of cellular interaction phenomena. Surf Sci Rep 29:1–30.

Rosoff WJ, Urbach JS, McAllister RG, Esrick MA, Richards LJ, Goodhill GJ. 2004. A novel chemotaxis assay reveals the extreme sensitivity of axons to molecular gradients. Nat Neurosci 7:678–682.

Wexler HM, Molitoris E, Murray PR, Washington J, Zabransky RJ, Edelstein PH, Fine-gold SM. 1996. Comparison of spiral gradient endpoint and agar dilution methods for susceptibility testing of anaerobic bacteria: A multilaboratory collaborative evaluation. J Clin Microbiol 34(1):170–174.